



## Ethyl malonate amides: A diketo acid offspring fragment for HIV integrase inhibition

Katarzyna Serafin<sup>a</sup>, Pawel Mazur<sup>a</sup>, Andrzej Bak<sup>a</sup>, Elodie Laine<sup>b</sup>, Luba Tchertanov<sup>b</sup>, Jean-François Mouscadet<sup>b</sup>, Jaroslaw Polanski<sup>a,\*</sup>

<sup>a</sup> Institute of Chemistry, University of Silesia, PL-40006 Katowice, Poland

<sup>b</sup> LBPA, Ecole Normale Supérieure de Cachan, CNRS, France

### ARTICLE INFO

#### Article history:

Received 19 May 2011

Revised 16 June 2011

Accepted 18 June 2011

Available online 29 June 2011

#### Keywords:

HIV integrase inhibitors

DKA

Ethyl malonate amide

### ABSTRACT

While searching for new HIV integrase inhibitors we discovered that some ethyl malonate amides (EMA) are active against this enzyme. Surprisingly, the main function can only very rarely be found among the reported drug candidates. We synthesised a series of compounds in order to establish and analyse the structure–activity relationship. The similarity to the important classes of HIV integrase inhibitors as well as the synthetic availability of the different targets including this pharmacophore makes EMA compounds an interesting object of investigations.

© 2011 Elsevier Ltd. All rights reserved.

### 1. Introduction

Fragmental approaches (FBA) to drug design that insist on the importance of low molecular frameworks are becoming more and more popular in medicinal chemistry.<sup>1</sup> A variety of FBA methods have been developed,<sup>2</sup> starting from the highly sophisticated screening of potential fragments by probing molecular recognition interaction using NMR studies of drug–ligand complexes to purely theoretical methods where low-molecular weight fragments make computations faster and more reliable.<sup>3,4</sup> Both appear to be useful in the construction of active compounds, regardless of the relatively low level of affinity of the starting motifs.<sup>5</sup>

Anti-AIDS therapy, which is an example of politargeted pharmacology based on different ligands, is probably one of the first approaches in clinics where a cocktail treatment against many viral targets has proved to be relatively successful. Although HIV integrase (IN) was early on found to be an attractive target for potential treatment, the first commercial IN directed drug, raltegravir, was not registered until 2007.<sup>6–9</sup> IN catalyses the insertion of reverse transcribed viral DNA into the host cell genome in two distinct steps: 3'-processing and strand transfer (ST). Enzyme action can result in the full integration of viral DNA and the host cell.

The discovery of the so-called diketo acid (DKA) pharmacophore appeared to be a turning point in the development of efficient IN inhibitors. Further modifications brought promising drug candidates that held up to clinical trial level.<sup>8</sup> Raltegravir also includes

the DKA fragment (Fig. 1). While searching for IN inhibitors, we discovered that some ethyl malonate amides (EMA) are active against this enzyme.

In Figure 1 we illustrated the fragmental similarity between the EMA function included in the investigated compounds and the DKA pharmacophore in raltegravir. The EMA fragment can only very rarely be found among the compounds investigated as potential IN inhibiting agents. In this publication we describe the results of the synthesis and biological evaluation of a series of EMA compounds that allowed us to analyse the structure–activity relationship. The fragment-based similarity to the important classes of HIV IN inhibitors was investigated using the database mining method.<sup>10,11</sup> The correspondence to raltegravir as well as the synthetic availability of different targets incorporating the EMA fragment makes it an interesting object for further modification.

### 2. Results and discussion

#### 2.1. Drug design

We tested fragments related to quinolinecarboxylic acids (Figs. 2 and 3c) that we had previously attempted to optimise.<sup>12</sup> Although SQ compounds look similar to DKA, their IN inhibition mechanism appears to be different, and the activity of the compounds is lower in comparison to DKAs.<sup>7,12</sup> The most active SQ1 analogue appeared to be compound FZ41, which has an IC<sub>50</sub> value of 0.7 μM. In Figure 2 we present some previous attempts to impart DKA advantages into SQ compounds. Thus, we attempted to extend the carboxylic function within the original series SQ1<sup>6,13</sup> by the addition of carbonyl in

\* Corresponding author.

E-mail address: [polanski@us.edu.pl](mailto:polanski@us.edu.pl) (J. Polanski).

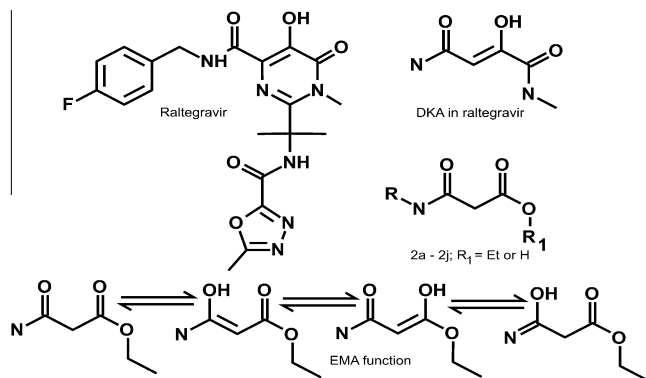


**Figure 1.** Fragmental similarity between EMA and raltegravir; different DKA tautomers were illustrated in the bottom.

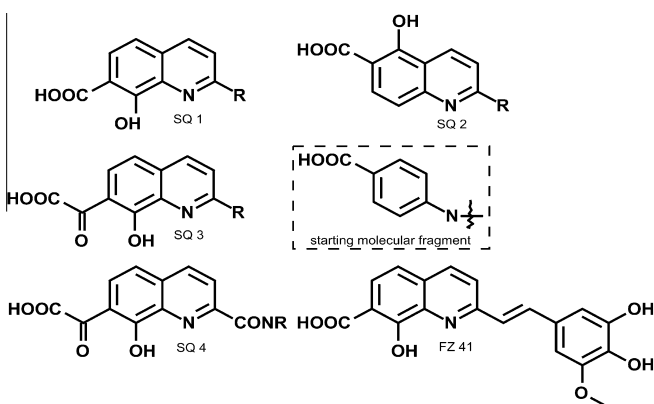


**Figure 2.** Modifications of the original series SQ1 to SQ2–SQ4 and SQ2 starting molecular fragment. Details in text.

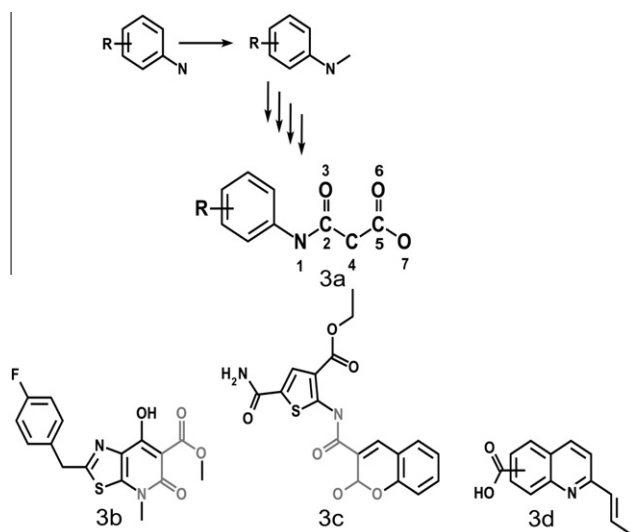


**Figure 3.** A construction scheme for the queries 3a used to mine the NIAID ChemDB anti-HIV database. The first fragment 1 is defined by the starting molecular fragment shown in Figure 2. Next, an incremental addition of the subsequent atoms 2–7 defined the successive queries. The frequencies of the database hits are listed in Table 1. Not a single hit including the whole EMA fragment was found. However, five hits (three within class 3b and two of the class 3c) were found for the EMA function masked within much more complex structures if deprived of aromatic substitution, as shown at the bottom. The SQ scaffold of the probed N to COOH arrangement is shown in (3d).

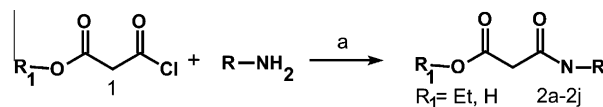
**Table 1**  
NIAID ChemDB hit frequency data for the EMA fragment

Aromatics	N <sup>1a</sup>	C <sup>2</sup>	O <sup>3</sup>	C <sup>4</sup>	C <sup>5</sup>	O <sup>6</sup>	O <sup>7</sup>
4-COOH	96	82	82	82	80	77	0
3-COOH	68	57	43	43	31	30	0
2-COOH	11 <sup>b</sup>	5 <sup>b</sup>	5 <sup>b</sup>	5 <sup>b</sup>	1 <sup>c</sup>	0	0

<sup>a</sup> 1254 Hits of the differently X substituted X-C<sub>6</sub>H<sub>4</sub>N fragment.

<sup>b</sup> Including three 2,4-isomers.

<sup>c</sup> 2,4-Isomer.



**Scheme 1.** Synthesis of EMA derivatives; (a) triethylamine, room temperature, stirred for 4 h.

SQ3<sup>14</sup> or carboxamide functions in SQ4,<sup>15</sup> as well as by modifying the carboxylic function arrangement SQ2. A fragmentation of FZ41 to SQ1 (R = CH<sub>3</sub>) drained all the potency from the original compound (IC<sub>50</sub> >100), while the activity of the isosteric fragment SQ2 (R = CH<sub>3</sub>) appeared higher having the IC<sub>50</sub> of 47 μM.<sup>16,17</sup>

Here we report the results of further fragmentation of SQ2 to find its potential active superstructure DKA constructs. We performed a data mining analysis of the NIAID ChemDB database collecting active compounds with a potential therapeutic action against HIV/AIDS.<sup>18</sup> The constructed fragments are defined in Figure 3 and the analysis of the database hits are shown in Table 1, which presents the detailed statistics of the occurrence of the sub-fragments analysed.

This analysis reveals the highest populated schemes for the molecular fragments related to the EMA function. Among 1254 hits containing fragment X-C<sub>6</sub>H<sub>4</sub>-N, where X means any substituent, 96 hits are 4-HOOC-C<sub>6</sub>H<sub>4</sub>-N- analogues, which also follows the activity changes within the SQ1 versus SQ2 fragment. Not a single hit including the whole EMA fragment was found; however, further fragmenting by subtraction of aromatics at N<sub>1</sub> revealed five hits that had the malonate amide fragment masked within the heterocyclic moieties as shown in Figure 3b and c, respectively.

## 2.2. Chemistry

All of the compounds studied were prepared according to Scheme 1, as was described previously.<sup>19</sup>

## 2.3. Biological activity

Inhibition of the HIV integrase was evaluated using short blunt-ended 21-mer U5B/U5A duplex oligonucleotides mimicking the viral U5 DNA extremity in the presence of 200 nM recombinant HIV-1 IN and 10 mM Mg<sup>2+</sup> ions. The results from the anti-integration activity assays are shown in Table 2. Compound 2a appeared to be the most active. The activity level of ca. 2 μM resembles that of the most active compounds including the MA fragment, namely, Figure 3b (from 35 to 1.23 μM)<sup>20</sup> and exceeds that of Figure 3c (56 or 90 μM).<sup>21</sup> Compounds 2b and 2c show only moderate activity while other compounds generally should be considered inactive. The analogy between EMA compounds and raltegravir revealed in Figure 1 suggests compound 2d, which has a (*p*-F-phenyl) methyl substitution on nitrogen as a fragment, most closely resembles raltegravir. However, this compound appeared to be inactive.

**Table 2**  
Inhibition of HIV-1 IN and calculated log *P* data for compounds **2a–2j**

No.	R	R <sub>1</sub>	IC <sub>50</sub> (μM)	log <i>P</i>
<b>2a</b>		Et	2	1.43
<b>2b</b>		Et	42	1.76
<b>2c</b>		Et	50	2.01
<b>2d</b>		Et	>100	1.45
<b>2e</b>		H	>100	0.97
<b>2f</b>		Et	N	1.89
<b>2g</b>		Et	>300	1.12
<b>2h</b>		Et	N	1.50
<b>2i</b>		Et	>100	2.69
<b>2j</b>		Et	500	0.98
Control:				
FZ41			0.7	–
Raltegravir			0.005	–

#### 2.4. Molecular modelling study

We previously reported an analysis of the spatial arrangement of the carbonyl and hydroxyl groups in the β-ketoenol motif (O=C–C=C–OH) in crystallographic and modelled virtual data for a large number of DKA compounds.<sup>22–24</sup> A comparison of compound **2a** with raltegravir reveals some fragmental similarities to EMA (Fig. 1). In order to test the differences in the binding mode of these compounds, we performed a docking study whose results are presented in Table 3 and Figure 4. In this study we used two IN structures. The first is a theoretical model of the full length DNA–IN complex obtained from 1WKN PDB entry. It represents the preintegration complex (PIC) which was commonly used as a molecular target for prospective inhibitors.<sup>25</sup> Compound **2a** was docked into

**Table 3**  
Results of the docking study

Compound	London function	Interacting residues <sup>a</sup>
<b>2a</b>	–11.01	C65, D64, D116, E152 <sup>**</sup>
Raltegravir	–19.18	C65, D,64, D116, E152 <sup>*</sup>

<sup>a</sup> Results of molecular docking.

<sup>\*</sup> Depicted on 2D receptor–ligand interaction diagram on Figure 4b and c.

<sup>\*\*</sup> Depicted in 3D mode on Figure 4a.

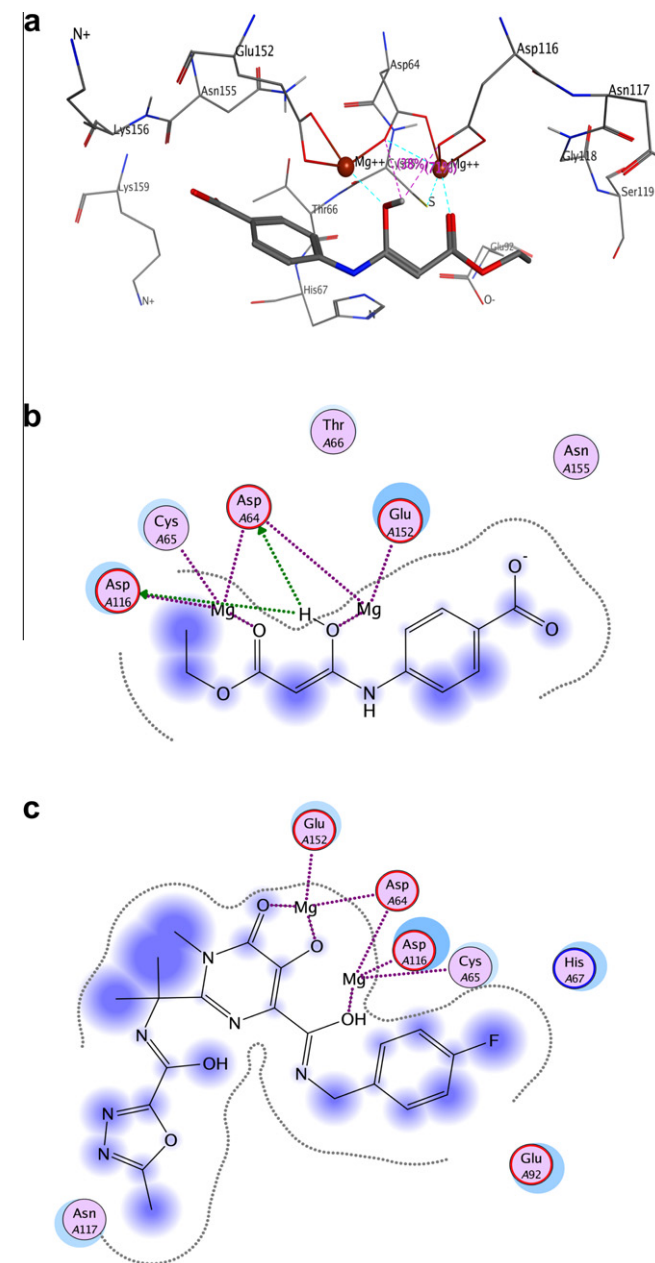


**Figure 4.** Compound **2a** docked within the 1WKN IN binding site, (a) two-dimensional plots comparing the interactions of individual IN residues with compound **2a** (b) and raltegravir (c).

the active site of the enzyme (DDE motif) of the PIC structure in a mode similar to raltegravir. The compounds are connected by the DKA group to DDE motif of IN via two ions of magnesium, which is believed to be one of the best arrangements. Raltegravir bonds are stronger because the inhibitor is connected via three

oxygen atoms as opposed to **2a** which lacks a complete DKA motif. Remarkably, the CYS65 is identified as an important counter-part in IN. This compares well to the results described in the literature.<sup>26,27</sup> Additionally, the analogues of **2a** (**2b–2j**) were docked into the active site of the PIC structure. Molecules **2c**, **2f** and **2i** are connected with DDE IN fragment employing only one magnesium cation. However, the other molecules generally reveal similar binding interactions which favourably promote the EMA motif, while the obtained values of London scoring function do not explain the loss of affinity compared to **2a**.

In Figure 5 we illustrate another simulation using 1WKN data in which we performed the superimposition of the EMA motif in compound **2a** and DKA pharmacophore moiety in the raltegravir molecule pre-docked to the IN. This was performed by covering six common atoms as detailed in Figure 5. The optimal overlap indicated by the relatively low RMSD value (RMS = 0.17 Å) was achieved for the amidol  $-N=C(OH)$  form of raltegravir and the  $\beta$ -ketoenol  $N-C(HO)=C-C=O$  motif of **2a** molecule. This forms provided also the best fit to the receptor.

Figure 6 represents the two-dimensional ligand–receptor plot which enables the qualitative study of the binding interactions of the superimposed **2a** molecule in two-dimensional HIV IN active side.

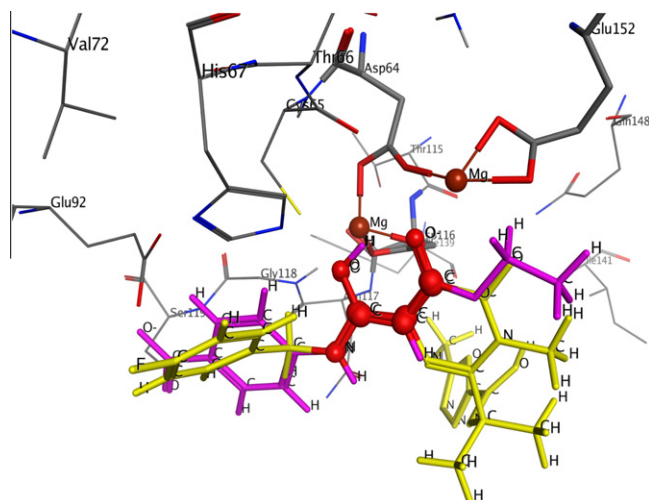


**Figure 5.** Compound **2a** superimposed on the docked raltegravir molecule. The circles indicate individual atoms specified for covering.

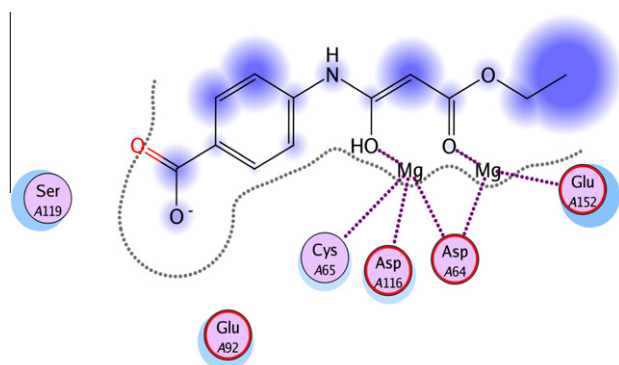


**Figure 6.** Two-dimensional diagram of the interactions of individual IN residues with the superimposed **2a** compound.

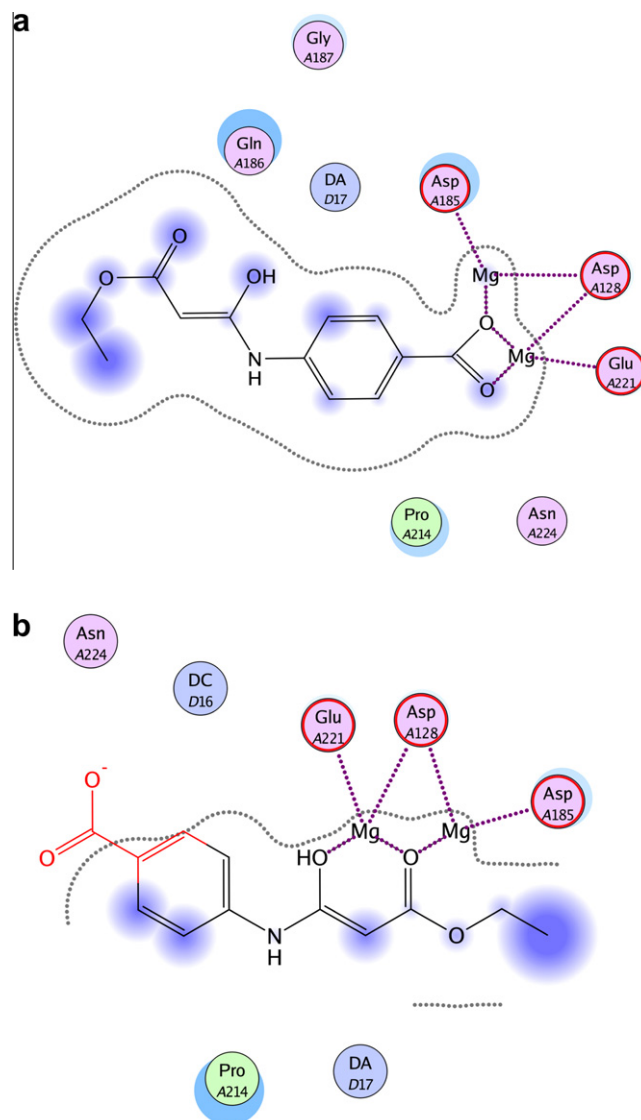


**Figure 7.** The two-dimensional plots comparing the interactions of individual PFV 30YA residues with compound **2a** docked within the binding site (a) and superimposed on the docked raltegravir (b) red color indicates the steric hindrance.

Despite the reverse orientation of the docked ( $LdG = -11.01$ ) and superimposed ( $LdG = -11.86$ ) molecule **2a** the same interacting mode was generally revealed, which indicates the crucial role of the EMA pattern. Not surprisingly, the docked orientations seem to be preferred due to the lack of the steric hindrance; however, it seems that both conformations were favorably connected with DDE motif of HIV IN employing two magnesium cations. Moreover, the molecular modelling of the DKA pharmacophore indicated that low-energy conformations might be equally well oriented in mutually reverse directions suggesting two potential binding modes, as was already revealed by the study of Hazuda et al.<sup>28</sup> Although the experimental structure of the HIV-1 intasome has not yet been determined, a co-crystal structure of the prototype foamy virus (PFV) intasome complexed with raltegravir (30YA pdb code) was reported recently.<sup>29</sup> Thus, we attempted to use this structure to dock compound **2a**. In contrast to the previous results, the binding characteristics of molecule **2a** do not show an agreement with the bound raltegravir, as is shown in Figure 7, namely, compound **2a** cannot meet the binding site requirements due to a steric hindrance.

## 2.5. Structure–activity relationship

The most active compound **2a** of the activity of 2  $\mu\text{M}$  resembles the activity level of methyl ester of 7-hydroxy-4-ethyl-5-oxo-4,5-dihydro-thiazolo[5,4-b]pyridine-6-carboxylic acid,<sup>20</sup> which also contains methyl malonate monoamide, a fragment closely related to the EMA one. The similarity of the EMA fragment to raltegravir is due to the methyl terminus  $\text{CH}_2\text{CH}_3$  (compound **2a**) or  $\text{NCH}_3$  (raltegravir), which is common to both compounds (Fig. 1). However, when we tried to bring this similarity even closer by adding aromatics to compound **2d** in order to imitate that of raltegravir, the compound was deprived of activity. The docking experiments that were performed using two different target structures reveal a better fit of raltegravir versus compound **2a**, which either suffers from an incomplete DKA function (1WKX) or steric hindrance (PFV 3OYA). The correspondence to important classes of HIV integrase inhibitors as well as the synthetic availability of the different targets including EMA makes the described compounds an interesting object for further investigations. Further insight into the EMA derivatives including structure- and ligand-based approaches might reveal new HIV IN inhibitors.

## 3. Conclusion

A series of ethyl malonate monoamides (EMA) synthesised as model compounds to test the influence of the aromatic fragment on the activity of SQ compounds appeared to be active. Mining the NIAID ChemDB Anti-HIV/OI/TB Therapeutics Database suggested fragments occurring preferentially within the compounds registered. It is interesting to observe that actually the high frequency fragment, namely, 4-HOOC-C<sub>6</sub>H<sub>4</sub>-N-, provided an active DKA offspring fragment, when used to construct EMA analogues.

## 4. Experimental

### 4.1. Molecular modeling and docking

Molecular modeling was conducted using the CCG MOE software packages<sup>30</sup> and the GNU/Linux Debian operating system. A structure of IN was prepared for docking by the addition of missing hydrogens, protein desolvation, calculation of atomic partial charges (AMBER99 force field) and the protonation of the protein at physiological pH 7.4 using the PROPKA related method. The ligands were constructed using the standard procedure including the structure optimisation with the MMFF94x force field and calculation of the partial atomic charges using the PM3 algorithm. Protomers and tautomers were generated for all compounds. We used the proxy triangle docking algorithm which performs the alignment of triplets of atoms on the triplets of the centres of alpha spheres created in the potential binding sites, in a systematic non-randomised way. In order to approximately evaluate the docking results, we used the London dG (LdG) scoring function (SF), which calculates the free energy of the binding of the ligand.<sup>31</sup> Two-dimensional plots of the ligand-IN interactions provided a schematic view of the 3D models simulated.

### 4.2. Synthesis

#### 4.2.1. General procedure for the synthesis of compounds 2a–2j

Amides **2a–2j** were prepared using a modified procedure as previously described.<sup>21</sup> Ethyl malonyl chloride (11 mmol) was added to a solution of aniline (10 mmol) in acetone. The reaction mixture was stirred for 4 h at room temperature and the solvent was removed *in vacuo*. Water was added to the residue and acidified with HCl to pH 3.

#### 4.2.2. 4-(2-Ethoxycarbonyl-acetylamino)benzoic acid, 2a

Yield 86% of white solid; mp 205 °C (lit. mp 204 °C<sup>21</sup>); <sup>1</sup>H NMR (DMSO-*d*<sub>6</sub>)  $\delta$  1.2 (t, *J* = 7.1, 3H, CH<sub>3</sub>); 3.48 (s, 2H, CH<sub>2</sub>); 4.1 (m, 2H, O-CH<sub>2</sub>); 7.6 (d, *J* = 8.7, 2H, Ar-H); 7.8 (d, *J* = 8.6, 2H, Ar-H); 10.5 (s, 1H, N-H); 12.7 (s, 1H, OH); LSI-MS (M+H)<sup>+</sup> = 252.2. Anal. Calcd for C<sub>12</sub>H<sub>13</sub>NO<sub>5</sub>: C, 57.37; H, 5.22; N, 5.58; O, 31.84. Found: C, 56.93; H, 5.72; N, 5.19; O, 31.1.

#### 4.2.3. N-(8-Hydroxy-quinolin-2-yl)-malonamic acid ethyl ester, 2b

Yield 36% of white solid; mp 125 °C; <sup>1</sup>H NMR (DMSO-*d*<sub>6</sub>)  $\delta$  1.2 (t, *J* = 7.1, 3H, CH<sub>3</sub>); 3.7 (s, 2H, CH<sub>2</sub>); 4.12 (m, 2H, O-CH<sub>2</sub>); 6.96 (d, *J* = 8.42, 1H, Ar-H); 7.1 (t, *J* = 7.7, 1H, Ar-H); 7.35 (d, *J* = 8.33, 1H, Ar-H); 7.5 (d, *J* = 7.87, 1H, Ar-H); 8.05 (s, 1H, O-H); 8.2 (d, *J* = 8.57, 1H, Ar-H); 8.5 (s, 1H, N-H); LSI-MS (M+H)<sup>+</sup> = 275.3. Anal. Calcd for C<sub>14</sub>H<sub>14</sub>N<sub>2</sub>O<sub>4</sub>: C, 61.31; H, 5.14; N, 10.21; O, 23.3. Found: C, 60.08; H, 5.72; N, 10.11; O, 23.62.

#### 4.2.4. N-*p*-Tolyl-malonamic acid ethyl ester, 2c

Yield 62% of white solid; mp 87 °C (lit. mp 86 °C<sup>32</sup>); <sup>1</sup>H NMR (DMSO-*d*<sub>6</sub>)  $\delta$  1.2 (t, *J* = 7.1, 3H, CH<sub>3</sub>); 2.24 (s, 3H, CH<sub>3</sub>-Ar); 3.42 (s, 2H, CH<sub>2</sub>); 4.1 (m, 2H, O-CH<sub>2</sub>); 7.1 (d, *J* = 8.2, 2H, Ar-H); 7.4 (d, *J* = 8.2, 2H, Ar-H); 10.0 (s, 1H, N-H); LSI-MS (M+H)<sup>+</sup> = 222.3. Anal. Calcd for C<sub>12</sub>H<sub>15</sub>NO<sub>3</sub>: C, 65.14; H, 6.83; N, 6.33; O, 21.69. Found: C, 64.95; H, 6.98; N, 6.21; O, 21.84.

#### 4.2.5. N-(4-Fluoro-benzyl)-malonamic acid ethyl ester, 2d

Yield 46% of white solid; mp 126–128 °C; <sup>1</sup>H NMR (DMSO-*d*<sub>6</sub>)  $\delta$  1.2 (t, *J* = 7.1, 3H, CH<sub>3</sub>); 3.27 (s, 2H, CH<sub>2</sub>); 4.1 (m, 2H, O-CH<sub>2</sub>); 4.2 (s, 2H, CH<sub>2</sub>); 7.1 (d, *J* = 8.6, 2H, Ar-H); 7.3 (d, *J* = 8.8, 2H, Ar-H); 8.5 (s, 1H, N-H); LSI-MS (M+H)<sup>+</sup> = 240.2. Anal. Calcd for C<sub>12</sub>H<sub>14</sub>FNO<sub>3</sub>: C, 60.24; H, 5.90; F, 7.94; N, 5.85; O, 20.05. Found: C, 60.01; H, 6.15; F, 7.83; N, 5.67; O, 20.37.

#### 4.2.6. N-(4-Methyl-2-nitro-phenyl)-malonamic acid, 2e

Yield 72% of white solid; mp 206 °C <sup>1</sup>H NMR (DMSO-*d*<sub>6</sub>)  $\delta$  3.48 (s, 2H, CH<sub>2</sub>); 7.6 (d, *J* = 8.7, 2H, Ar-H); 7.8 (d, *J* = 8.6, 2H, Ar-H); 10.5 (s, 1H, N-H); 12.7 (s, 2H, OH); LSI-MS (M+H)<sup>+</sup> = 238.1. Anal. Calcd for C<sub>11</sub>H<sub>13</sub>NO<sub>5</sub>: C, 55.23; H, 5.48; N, 5.85; O, 33.44. Found: C, 55.11; H, 5.62; N, 5.98; O, 33.62.

#### 4.2.7. N-(4-Methyl-2-nitro-phenyl)-malonamic acid ethyl ester, 2f

Mp 62–64 °C (lit. mp 60 °C).<sup>33</sup>

#### 4.2.8. 3-(2-Ethoxycarbonyl-acetylamino)-4-hydroxy-benzoic acid, 2g

Yield 63% of white solid; mp 179 °C; <sup>1</sup>H NMR (DMSO-*d*<sub>6</sub>)  $\delta$  1.2 (t, *J* = 7.1, 3H, CH<sub>3</sub>); 3.59 (s, 2H, CH<sub>2</sub>); 4.12 (m, 2H, O-CH<sub>2</sub>); 6.92 (d, *J* = 8.44, 1H, Ar-H); 7.56 (d, *J* = 8.41, 1H, Ar-H); 8.56 (s, 1H, Ar-H); 9.56 (s, 1H, N-H); 10.79 (s, 1H, OH); LSI-MS (M+H)<sup>+</sup> = 284.24. Anal. Calcd for C<sub>12</sub>H<sub>13</sub>NO<sub>7</sub>: C, 50.89; H, 4.63; N, 4.95; O, 39.54. Found: C, 50.2; H, 4.81; N, 5.19; O, 39.93.

#### 4.2.9. N-(2-Nitro-phenyl)-malonamic acid ethyl ester, 2h

Mp 89–91 °C (lit. mp 89 °C).<sup>34</sup>

#### 4.2.10. N-(2,6-Dichloro-phenyl)-malonamic acid ethyl ester, 2i

Yield 62% of brown solid; mp 116 °C; <sup>1</sup>H NMR (DMSO-*d*<sub>6</sub>)  $\delta$  1.2 (t, *J* = 7.1, 3H, CH<sub>3</sub>); 3.47 (s, 2H, CH<sub>2</sub>); 4.1 (m, 2H, O-CH<sub>2</sub>); 7.35 (t, *J* = 8.15, 1H, Ar-H); 7.53 (d, *J* = 8.12, 2H, Ar-H); 10.11 (s, 1H, N-H); LSI-MS (M+H)<sup>+</sup> = 290.15. Anal. Calcd for C<sub>12</sub>H<sub>13</sub>Cl<sub>2</sub>NO<sub>3</sub>: C, 49.68; H, 4.52; Cl, 24.44; N, 4.83; O, 16.54. Found: C, 49.1; H, 4.83; Cl, 23.92; N, 4.71; O, 16.83.

#### 4.2.11. 3-Oxo-3-(toluene-4-sulfonylamino)-propionic acid ethyl ester, 2j

Mp 97–98 °C (lit. mp 98 °C).<sup>35</sup>

All reagents were purchased from Aldrich. Kieselgel 60, 0.040–0.063 mm (Merck, Darmstadt, Germany) was used for column chromatography. TLC experiments were performed on alumina-backed silica gel 40 F254 plates (Merck, Darmstadt, Germany). The plates were illuminated under UV (254 nm) and evaluated in iodine vapour. The melting points were determined on a Boetius PHMK 05 instrument (VEB Kombinat Nagem, Radebeul, Germany) and are uncorrected. Elemental analyses were carried out on an automatic Perkin-Elmer 240 microanalyser (Boston, USA) for C, H, N and are within 0.4% of theoretical values. The purity of the final compounds was checked using TLC. All <sup>1</sup>H NMR spectra were recorded on a Bruker AM-500 (499.95 MHz for <sup>1</sup>H), Bruker BioSpin Corp., Germany. Chemical shifts are reported in ppm ( $\delta$ ) against the internal standard, Si(CH<sub>3</sub>)<sub>4</sub>. Easily exchangeable signals were omitted when diffuse.

Melting points were measured in an open capillary on an Opti-Melt (SRS) melting point apparatus and are uncorrected. <sup>1</sup>H NMR spectra were recorded at 400 MHz in DMSO solutions on a Bruker UltraShield™ NMR spectrometer. The chemical shifts are as parts per million ( $\delta$  ppm) from TMS as an internal standard. ESI-MS were determined using a Varian 500-MS mass spectrometer and signals were recorded in *m/z*. Elemental analysis was performed using a Perkin-Elmer CHNS/O Series II 2400 elemental analyser.

#### 4.3. Biological activity measurements

IN was expressed and purified as described previously.<sup>36</sup> For activity assays, 100 pmol of U5B were radiolabelled using T4 polynucleotide kinase and 50 Ci of [<sup>32</sup>P]ATP (3000 Ci/mmol). The T4 kinase was then heat-inactivated, and unincorporated nucleotides were removed by filtration through a Sephadex G-25 column (Amersham Biosciences AB, Uppsala, Sweden). NaCl was added to a final concentration of 100 mM and the complementary unlabeled strand U5A was added. The mixture was incubated at 90 °C for 3 min and allowed to anneal by slowly cooling to room temperature. The 3-processing and strand transfer reactions were performed using 1.5 nM U5A/U5B and 10 nM U5A double-stranded oligonucleotide substrates, respectively, in a buffer containing 20 mM HEPES, pH 6.8, 7.5 mM MgCl<sub>2</sub>, and 2 mM DTT in the presence of various concentrations of IN. The reaction mixture was incubated for 1 h at 37 °C and stopped by phenol–chloroform extraction. Chemical structures were dissolved in DMSO and subjected to electrophoresis on an 18% denaturing acrylamide/urea gel. Gels were dried and the reaction products were visualized using a STORM PhosphorImager (Amersham Biosciences). IC<sub>50</sub> were obtained from a nonlinear regression fitting of the dose–response curves using IMAGE QUANT TL software.

#### Acknowledgments

This study is supported by grants from the Polish Ministry of Science N405 178735 and NN519 575638.

#### References and notes

- Rees, D. C.; Congreve, M.; Murray, C. W.; Carr, R. *Nat. Rev. Drug Discov.* **2004**, *3*, 660.
- Hajduk, P. J.; Greer, J. *Nat. Rev. Drug Discov.* **2007**, *6*, 211.
- Law, R.; Barker, O.; Barker, J. J.; Hesterkamp, T.; Godemann, R.; Andersen, O.; Fryatt, T.; Courtney, S.; Hallett, D.; Whittaker, M. *J. Comput. Aided Mol. Des.* **2009**, *23*, 459.
- Chen, Y.; Shoichet, B. K. *Nat. Chem. Biol.* **2009**, *5*, 358.
- Bartoli, S.; Fincham, C. I.; Fattori, D. *Curr. Opin. Drug Discov. Dev.* **2007**, *10*, 422.
- Mekouar, K.; Mouscadet, J. F.; Desmaële, D.; Subra, F.; Leh, H.; Savouré, D.; Auclair, C.; d'Angelo, J. *J. Med. Chem.* **1998**, *41*, 2846.
- Pommier, Y.; Johnson, A. A.; Marchand, C. *Nat. Rev. Drug Discov.* **2005**, *4*, 236.
- Luo, Z. G.; Tan, J. J.; Zeng, C. X.; Hu, L. M. *Mini-Rev. Med. Chem.* **2010**, *10*, 1046.
- Ramkumar, K.; Neamati, N. *Core Evid.* **2010**, *15*, 131.
- Chen, J. H.; Linstead, E.; Swamidass, S. J.; Wang, D.; Baldi, P. *Bioinformatics* **2007**, *23*, 2348.
- Grzybowski, B. A.; Bishop, K. J.; Kowalczyk, B.; Wilmer, C. E. *Nat. Chem.* **2009**, *1*, 31.
- Mouscadet, J. F.; Desmaële, D. *Molecules* **2010**, *15*, 3048.
- Polanski, J.; Zouhiri, F.; Jeanson, L.; Desmaële, D.; d'Angelo, J.; Mouscadet, J. F.; Gieleciak, R.; Gasteiger, J.; Le Bret, M. *J. Med. Chem.* **2002**, *45*, 4647.
- Maurin, C.; Bailly, F.; Mbemba, G.; Mouscadet, J. F.; Cotelle, P. *Bioorg. Med. Chem.* **2006**, *14*, 2978.
- Bénard, C.; Zouhiri, F.; Normand-Bayle, M.; Danet, M.; Desmaële, D.; Leh, H.; Mouscadet, J. F.; Mbemba, G.; Thomas, C. M.; Bonnenfant, S.; Le Bret, M.; d'Angelo, J. *Bioorg. Med. Chem. Lett.* **2004**, *17*, 2473.
- Polanski, J.; Niedbala, H.; Musiol, R.; Podeszwa, B.; Tabak, D.; Palka, A.; Mencil, A.; Finster, J.; Mouscadet, J. F.; Le Bret, M. *Let. Drug Des. Discov.* **2006**, *3*, 175.
- Polanski, J.; Niedbala, H.; Musiol, R.; Podeszwa, B.; Tabak, D.; Palka, A.; Mencil, A.; Mouscadet, J. F.; Le Bret, M. *Let. Drug Des. Discov.* **2007**, *4*, 99.
- ChemDB anti-HIV. Available at: <<http://www.chemdb.niaid.nih.gov/>>.
- Ukrainets, I.; Bezugly, P.; Treskach, V.; Taran, S.; Gorokhova, O. *Tetrahedron* **1994**, *50*, 10331.
- Boros, E. E.; Johns, B. A.; Garvey, E. P.; Koble, C. S.; Miller, W. H. *Bioorg. Med. Chem. Lett.* **2006**, *16*, 5668.
- Deng, J.; Sanchez, T.; Neamati, N.; Briggs, J. M. *J. Med. Chem.* **2006**, *49*, 1684.
- Tchertanov, L.; Mouscadet, J. F. *J. Med. Chem.* **2007**, *50*, 1133.
- Bak, A.; Magdziarz, T.; Kurczyk, A.; Polanski, J. *Drug Dev. Res.* **2011**, *72*, 209.
- Bak, A.; Magdziarz, T.; Kurczyk, A.; Polanski, J. *Comb. Chem. High Throughput Screen* **2011**, *14*, in press.
- Hare, S.; Vos, A. M.; Clayton, R. F.; Thuring, J. W.; Cummings, M. D.; Cherepanov, P. *PNAS* **2010**, *107*, 20057.
- Savarino, A. *Retrovirology* **2007**, *20*, 4.
- Loizidou, E. Z.; Zenelipour-Yazdi, C. D.; Christofides, T.; Kostrikis, L. G. *Bioorg. Med. Chem.* **2009**, *17*, 4806.
- Hazuda, J. D.; Anthony, N. J.; Gomez, R. P.; Jolly, S. M.; Wai, J. S.; Zhuang, L.; Fisher, T. E.; Embrey, M.; Guare, J. P.; Egbertson, M. S.; Vacca, J. P.; Huff, J. R.; Felock, P. J.; Witmer, M. V.; Stillmock, K. A.; Danovich, R.; Grobler, J.; Miller, M. D.; Espeseth, A. S.; Jin, L.; Chen, I. W.; Lin, J. H.; Kassahun, K.; Ellis, J. D.; Wong, B. K.; Xu, W.; Pearson, P. G.; Schleif, W. A.; Cortese, R.; Emini, E.; Summa, V.; Holloway, M. K.; Young, S. D. *PNAS* **2004**, *101*, 11233.
- Hare, S.; Gupta, S. S.; Valkov, E.; Engelman, A.; Cherepanov, P. *Nature* **2010**, *464*, 232.
- Molecular Operating Environment (MOE 2008.10), CCG Inc., 1255 University St., Suite 1600, Montreal, Quebec, Canada H3B 3X3. <<http://www.chemcomp.com/>>.
- Mazur, P.; Magdziarz, T.; Bak, A.; Chilmonczyk, Z.; Kasprzycka-Guttman, T.; Misiewicz, I.; Skupinska, J.; Polanski, J. *J. Mol. Model.* **2010**, *16*, 1205.
- Jeon, M. K.; Kim, K. *Tetrahedron Lett.* **2002**, *43*, 3415.
- Fusco, R.; Rossi, S. *Gazzetta Chimica Italiana* **1964**, *94*, 3.
- Chakraborty, K.; Devakumar, C. *J. Agric. Food Chem.* **2006**, *54*, 6800.
- Morzherin, Y.; Rozin, Y.; Vorobeva, E.; Bakulev, V. *Chem. Heterocycl. Compd.* **2001**, *37*, 560.
- Hazuda, D. J.; Hastings, J. C.; Wolfe, A. L.; Emini, E. A. *Nucleic Acids Res.* **1994**, *22*, 1121.